CHIN. PHYS. LETT. Vol. 34, No. 6 (2017) 063701

# Measurement of Heating Rates in a Microscopic Surface-Electrode Ion Trap *

Jiu-Zhou He(何九洲)[1,2], Lei-Lei Yan(闫磊磊)[1,2], Liang Chen(陈亮)[1**], Ji Li(李冀)[1,2], Mang Feng(冯芒)[1**]

[1]*State Key Laboratory of Magnetic Resonance and Atomic and Molecular Physics, Wuhan Institute of Physics and Mathematics, Chinese Academy of Sciences, Wuhan 430071*

[2]*University of the Chinese Academy of Sciences, Beijing 100049*

(Received 19 January 2017)

*We report measurement of heating rates of $^{40}Ca^{+}$ ions confined in our home-made microscopic surface-electrode trap by a Doppler recooling method. The ions are trapped with approximately 800 μm above the surface, and are subjected to heating due to various noises in the trap. There are 3–5 ions involved to measure the heating rates precisely and efficiently. We show the heating rates in variance with the number and the position of the ions as well as the radio-frequency power, which are helpful for understanding the trap imperfection.*

*PACS:* 37.10.Ty, 03.67.Lx, 41.20.−q DOI: 10.1088/0256-307X/34/6/063701

Trapped ions in a harmonic potential constitute a promising candidate for quantum information processing. Since scalability of the ions requires exact manipulation of both the spins and positions of the qubits, fast and coherently moving the ions becomes an essential task. The simplest way to this end is to build multi-electrode architecture with the confined ions moving back and forth under the control. So far, developing planar ion traps with all the electrodes lying within a plane has been carried out in several groups in the world.[1−6]

The main detrimental factor in the trap is the ambient motional decoherence caused by thermal electronic noise in the resistance of the electrodes or resistance coupled to the electrodes. For the ions experiencing relatively low oscillation frequencies, the ambient decoherence is normally described by the Johnson noise, a kind of thermal noise associated with lumped circuit elements attached to the electrodes, or equivalently, thermally fluctuating dipole oscillators in the electrode bulk.[7,8] As a result, with the ions closer to the electrodes, the ions are more easily heated, which causes the confinement instability and also leads to decoherence of the spin states.[8] Under the Johnson noise, the typical heating rates, expressed as quanta per second from the motional ground state, are observed to be around $d\langle n\rangle/dt = 10^3$–$10^4\,\mathrm{s}^{-1}$ for the oscillation frequency of the order of tens of MHz and the distance from the ion to the nearest electrode surface around 150 μm. However, for some planar multi-electrode architectures, the observed electric field noise can be three orders of magnitude larger than that expected from the Johnson noise consideration, which is called anomalous heating. The principal cause of the anomalous heating is not understood at the moment, but some of its characteristics have been summarized. The fluctuating field from the electrodes themselves has no sharp spectral features in the range from 2 to 20 MHz. Based on the observations of different ions,[9−12] this heating effect might be relevant to the surface effect itself, the contamination on the electrodes or some other unknown noise sources.[13−16] The latest works have shown that the above-mentioned noise can be suppressed by operating traps at cryogenic temperatures[17] and removing the surface contaminants using laser ablation cleaning is an effective way.[10] Those methods have reduced the heating rates by at least two orders of magnitude.

Exploring the anomalous heating in the ion trap is helpful for beating decoherence of qubits, and can also provide an effective means as a nanoscale probe for material science research.[18,19] To measure the heating rate, we may detect the number of phonons changing with time[8] after the ions have been cooled down to the ground state of the vibration. Alternatively, we consider the Doppler recooling method,[20] which is valid for the hot ions under strong heating. Since the heating rate scales with the separation $d$ between the ion and the nearest electrode by $d^{-4}$, an exact measurement of the heating rate requires a small value of $d$. For the surface-electrode trap, the Doppler recooling method generally works for the trapping height of the ions less than 200 μm.

In this Letter, we report our measurements of heating rates in our home-made microscopic surface-electrode (MSE) trap by the Doppler recooling method. In our case, since the $^{40}Ca^{+}$ ions are confined in a distance of 800 μm from the surface, we make the measurement by increasing the number of the ions to improve the sensitivity and the precision. We also analyze the influence from the radio-frequency (rf) field and the heating at different positions in the trap. Our purpose is to understand the imperfection of the trap and to explore the possibility of trapped

*Supported by the National Natural Science Foundation of China under Grant Nos Y5Z2111001, 91421111 and 11674360.

**Corresponding author. Email: liangchen@wipm.ac.cn; mangfeng@wipm.ac.cn

ions as a nanoscale probe for metal surface.

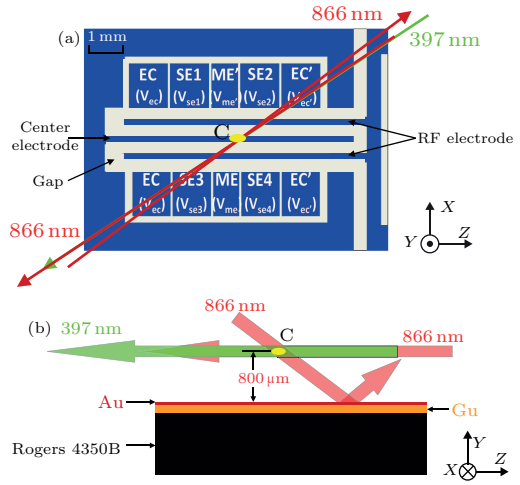


**Fig. 1.** Schematic drawing of our MSE trap in top view along the $y$ direction (a) and side view in the $x$ direction (b), showing a central electrode, two rf electrodes and two outer segmented dc electrodes. The letters marked in the two outer segmented dc electrodes are the names of the dc electrodes and the letters in the brackets are the corresponding voltages. The yellow dot C labels the position of the trapped ions located at about 800 μm above the surface of MSE trap. The green and red arrows in (a) and (b) indicate the orientation of the cooling (397 nm) laser and the repumping (866 nm) laser, respectively. The substrate is made of a printed circuit board (PCB) with copper electrodes covered by gold.

As shown in Fig. 1, our MSE trap is a 500 μm scale planar trap with five electrodes, including a central electrode, two rf electrodes and two outer segmented dc electrodes. The electrodes are made of copper on a vacuum-compatible PCB substrate. The copper electrodes are of thickness of 35 μm and covered by a 5-μm-thick gold layer. The radially confining potential $\Phi_{\rm rf}(x,y,z)$[12,21] is produced by the two rf electrodes with the amplitude and frequency of the rf voltage being $V_{\rm rf} \sim 400$ V (0-peak) and $\Omega_{\rm rf}/2\pi = 22$ MHz, respectively. The axially confining potential $\Phi_{\rm dc}(x,y,z)$ is produced by the four end-cap (EC) electrodes whose voltage is $V_{\rm ec} = 40$ V, and other electrodes are grounded. The net pseudopotential $\Psi(x,y,z)$ is the sum of radial and axial potentials,[21,22]

$$\Psi(x,y,z) = \frac{Q^2}{4m\Omega_{\rm rf}^2}|\nabla\Phi_{\rm rf}(x,y,z)|^2 + Q\Phi_{\rm dc}(x,y,z), \quad (1)$$

where $Q$ and $m$ are the corresponding charge and mass of the ions, and the secular motion frequencies in $x$, $y$ and $z$ directions are $\omega_{x,y,z}/2\pi = 531.9$, 818.3 and 183.7 kHz, respectively.

Several lasers are employed in our case, for example, a 397 nm laser for the Doppler cooling with the power of 140 μW, a 866 nm laser for the D-state repumping with the power of 500 μW and a 423 nm radiation with the power of 200 μW for the photoionization of neutral calcium atoms. To keep the frequency stabilized, we lock the 397 nm and 866 nm lasers to an optical cavity made of a material with ultra-low expansion, and we also employ the Pound–Drever–Hall technique. The incident directions of the 397 nm and 866 nm lasers are parallel to the trap surface to avoid the laser beams striking the surface of the trap which may lead to the scattering light into the detectors and charging of the substrate. However, to cool the motion along the $y$ axis, we irradiate the 866 nm laser with a small angle of 3.8° with respect to the $x$–$z$ plane, which provides a small component of cooling effect in the $y$ axis.[6] The trapped ions can be detected by laser-induced fluorescence of 397 nm, which is split into two beams by a 30/70 beam-splitter and the fluorescence is collected by a photomultiplier tube (PMT) (9893QSB, ET Enterprises) and an electron-multiplying CCD (EMCCD) (Photon-Max512, Princeton Instruments). The 866 nm laser is controlled by an AOM 80-20 double pass.

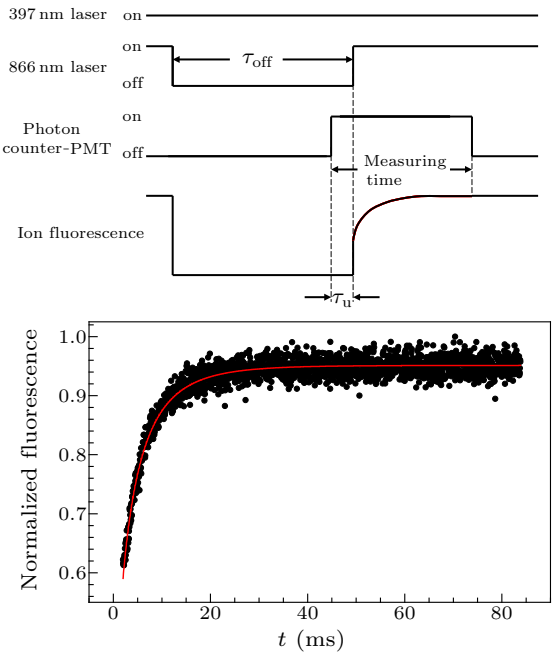


**Fig. 2.** (a) Schemes of the laser pulses and the PMT switching as well as the change of the fluorescence in our experiment, where $\tau_{\rm off}$ is the time period for turning off the 866 nm repumping laser and the multi-channel scaler starts before restoring the 866 nm laser by $\tau_{\rm u}$. (b) Normalized Doppler recooling curve for five ions with $\tau_{\rm off} = 100$ ms, where the data are accumulated by 300 times before normalized. The dots are the experimental values and the solid curve is from a fitting by Eq. (2).

The Doppler recooling method works by measuring the increased Doppler shift of the ions, which helps for estimating the ions' energy by assuming the instantaneous ion fluorescence as the steady-state fluorescence of the Doppler-cooled ions. To evaluate the change in fluorescence, we turn off the 866 nm repumping laser for a period of $\tau_{\rm off}$ during which the ions heat up, as shown in Fig. 2(a). The change in the ions' fluorescence is monitored as the ions are cooled down again

after the Doppler cooling restarts. This fluorescence change can be considered as the energy gain of the ions during $\tau_{\rm off}$ and thus we can deduce the ions' heating rate. The fluorescence data are recorded by the multi-channel scaler (SR430), which, for avoiding any data loss, is switched on before the fluorescence is restored. After removing the invalid data that the multi-channel scaler recorded during the time period of $\tau_{\rm u}$, we obtain the recooling curves, as shown in Fig. 2(b), where we exemplify a normalized fluorescence curve for five ions after heating for 100 ms.

To extract the ion energy from the recooling curves, we fit the observed data by the method proposed in Ref. [20] under the assumption that a harmonic oscillator owns the smallest projection of the three-ion modes with the projection along the laser beam. We thus refer to the quantity $\varepsilon$ as the scaled energy. The solid curve in Fig. 2(b) is fitted based on the scattering rate predicted by

$$\left\langle \frac{dN}{d\tau} \right\rangle_{\bar{\varepsilon}} = \int_0^\infty P_0(\varepsilon') \frac{dN}{d\tau}\Big|_{\varepsilon=\Xi(\varepsilon',\tau)} d\varepsilon', \qquad (2)$$

where $P_0(\varepsilon) = e^{-\varepsilon/\bar{\varepsilon}}/\bar{\varepsilon}$ is the Maxwell–Boltzmann distribution of the motional energies with the mean energy $\bar{\varepsilon}$ at the beginning of each cooling period, and $\Xi(\varepsilon', \tau)$ denotes the energy of an atom at time $\tau$ with energy $\varepsilon'$ at the initial time ($\tau = 0$). The scattering rate is given by $dN/d\tau = {\rm Im}(Z)/2\sqrt{\varepsilon r}$ with $Z = i/\sqrt{1-(\delta+i)^2/2\varepsilon r}$ and the energy $\varepsilon$ can be calculated by the change rate equation $d\varepsilon/d\tau = [{\rm Re}(Z) + \delta {\rm Im}(Z)]/2\sqrt{\varepsilon r}$ with the initial energy $\varepsilon'$ and $\delta = 2\Delta/\Gamma\sqrt{1+s}$. The parameters in our experiment are given by $\Delta/2\pi = -5$ MHz, $\Gamma/2\pi = 21$ MHz, $r = 0.0022$ and $s = 0.9$.

In the implementation of our experiment, the intensity of the 397 nm laser beam is actively stabilized at the value of 17.8 mW/mm$^2$, and the corresponding frequency is detuned from the transition of $S_{1/2} \longleftrightarrow {\rm P}_{1/2}$. The intensity of the 866 nm laser is adjusted at 50.9 mW/mm$^2$ with red-detuning by 5 MHz from the $D_{3/2} \longleftrightarrow {\rm P}_{1/2}$ transition. For our purpose, we employ a multi-channel scaler to record the fluorescence data, which possesses 2048 channels. The time bin of each channel is set to be 40 μs. We accumulate the data 300 times for each measurement, and repeat this measurement three times.

To investigate the heating rates in different situations, we change the heating time $\tau_{\rm off}$ from 50 ms to 150 ms with the step of 25 ms and consider the number of the ions from three to five. After repeating each procedure five times, we obtain five averaged data for each case with a certain number of ions, as shown in Fig. 3 where the slopes of the fitting lines are the heating rates of the ionic crystals. The observation indicates that heating in the trap increases linearly with the number of the ions. To understand the type of the noise we observed, we have also compared our values with those purely from the Johnson noise under an assumption that the three-ion case only experiences the Johnson noise. As plotted in Fig. 3(d), the additional noises are found in the cases of four and five ions, implying anomalous noise.

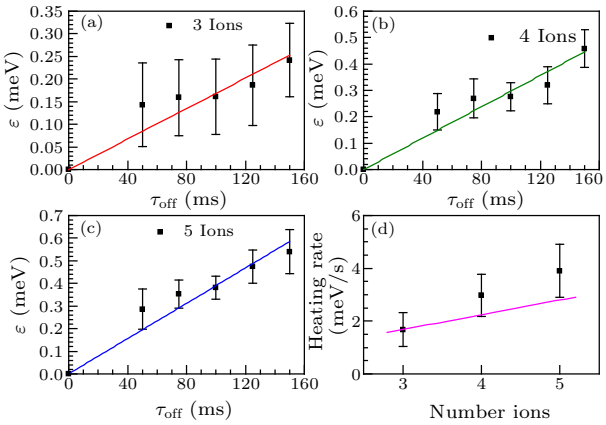


**Fig. 3.** Scaled energy $\varepsilon$ as a function of the heating time $\tau_{\rm off}$ in the Doppler recooling experiments. As is expected, the energy of the ions scales linearly with the heating time and a linear fit including the origin point indicates $d\varepsilon/dt$, implying the heating rate. The values for three to five ions are plotted, respectively, in (a)–(c). The heating rates calculated from (a)–(c) are plotted in (d) with respect to the number of the ions and compared with the Johnson noise (the purple line). The error bars are standard deviation for five repetitions of the measurement and the lines in (a)–(c) are fitted by the least square method.

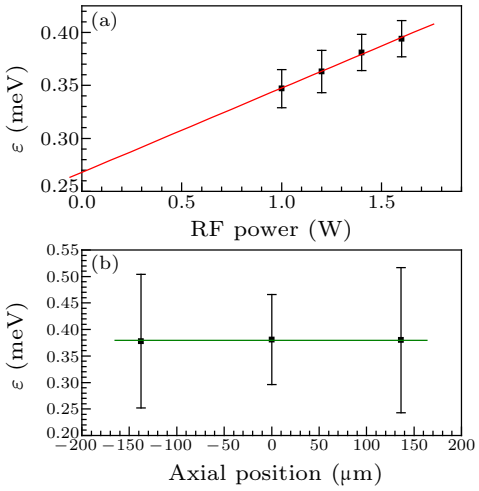


**Fig. 4.** (Upper panel) Scaled energy $\varepsilon$ for five ions as a function of the rf power. (Lower panel) Scaled energy $\varepsilon$ for five ions as a function of the ions' position. The heating time $\tau_{\rm off}$ is 100 ms, and the error bars are standard deviation for five repetitions of the measurement.

Part of the heating we observed comes from the rf field. Depending on the above parameters, we have calculated the rf potential null, which is above the trap surface about 910 μm. As such, the confined ions in our experiment surely are affected by the rf heating since they are not fully compensated to the rf-potential null. For this reason, we measure the energy of the ions under different rf powers from 1.0 W

to 1.6 W with the increase of 0.2 W. As shown in Fig. 4(a), the energy of the ions enlarges linearly with the rf power. Moreover, to understand the spatial feature of the trap, we have measured the heating energies at different positions in the trap. Starting with five ions from the trap center, we move the ions leftward and rightward by 136 and 137 μm, respectively. Figure 4(b) demonstrates the nearly constant heating rate with respect to different positions, implying a homogeneous noise in the trap.

In summary, we have measured the heating rates with three to five ions in an MSE trap. The observations present clearly the variation of the heating in the trap with the number and position of the ions as well as the rf power applied. To our knowledge, this is the first work in China to explore the anomalous noise in the ion trap, which is complex and multifaceted, and depends on the trap material or the type and coverage fraction of surface impurities. To further clarify the origin of the noise, we reduce the electrodes' size for achieving a smaller distance between the ions and the surface and for a better compensation to the rf-potential null. Therefore, the present results start the way to understanding the real trap potential more deeply, confining the ion crystals more reasonably and implementing quantum control of the ions more precisely.

## References


[1] Chiaverini J, Blakestad R B, Britton J, Jost J D, Langer C, Leibfried D, Ozeri R and Wineland D J 2005 *Quantum Inf. Comput.* **5** 419

[2] Seidelin S, Chiaverini J, Reichle R, Bollinger J J, Leibfried D, Britton J, Wesenberg J H, Blakestad R B, Epstein R J, Hume D B, Itano W M, Jost J D, Langer C, Ozeri R, Shiga N and Wineland D J 2006 *Phys. Rev. Lett.* **96** 253003

[3] Pearson C E, Leibrandt D R, Bakr W S, Mallard W J, Brown K R and Chuang I L 2006 *Phys. Rev.* A **73** 32307

[4] Labaziewicz J, Ge Y, Antohi P, Leibrandt D, Brown K R and Chuang I L 2008 *Phys. Rev. Lett.* **100** 13001

[5] Leibrandt D R, Labaziewicz J, Clark R J, Chuang I L, Epstein R J, Ospelkaus C, Wesenberg J H, Bollinger J J, Leibfried D, Wineland D J, Stick D, Sterk J, Monroe C, Pai C S, Low Y and Slusher R E 2009 *Quantum Inf. Comput.* **9** 0910

[6] Allcock D T C, Sherman J A, Stacey D N, Burrell A H, Curtis M J, Imreh G, Linke N M, Szwer D J, Webster S C and Steane A M 2010 *New J. Phys.* **12** 053026

[7] Turchette Q A, Kielpinski D, King B E, Leibfried D, Meekhof D M, Myatt C J, Rowe M A, Sackett C A, Wood C S, Itano W M, Monroe C and Wineland D J 2000 *Phys. Rev.* A **61** 063418

[8] Deslauriers L, Olmschenk S, Stick D, Hensinger W K, Sterk J and Monroe C 2006 *Phys. Rev. Lett.* **97** 103007

[9] Daniilidis N, Narayanan S, Möller S A, Clark R, Lee T E, Leek P J, Wallraff A, Schulz St, Schmidt-Kaler F and Häffner H 2011 *New J. Phys.* **13** 013032

[10] Allcock D T C, Guidoni L, Harty T P, Ballance C J, Blain M G, Steane A M and Lucas D M 2011 *New J. Phys.* **13** 123023

[11] Hite D A, Colombe Y, Wilson A C, Brown K R, Warring U, Jördens R, Jost J D, McKay K S, Pappas D P, Leibfried D and Wineland D J 2012 *Phys. Rev. Lett.* **109** 103001

[12] Charles D S, Amini J M, Wright K, Volin C, Killian T, Ozakin A, Denison D, Hayden H, Pai C S, Slusher R E and Harter A W 2012 *New J. Phys.* **14** 073012

[13] Wineland D J, Monroe C, Itano W M, Leibfried D, King B E and Meekhof D M 1998 *J. Res. Nat. Inst. Stand. Technol.* **103** 259

[14] Dubessy R, Coudreau T and Guidoni L 2009 *Phys. Rev.* A **80** 031402

[15] Guang H L, Herskind P F and Chuang I L 2011 *Phys. Rev.* A **84** 053425

[16] Brownnutt M, Kumph M, Rabl P and Blatt R 2015 *Rev. Mod. Phys.* **87** 1419

[17] Bruzewicz C D, Sage J M and Chiaverini J 2015 *Phys. Rev.* A **91** 041402

[18] Hite D A, Colombe Y, Wilson A C, Allcock D T C, Leibfried D, Wineland D J and Pappas D P 2013 *MRS Bull.* **38** 826

[19] Eltony A M, Park H G, Wang S X, Kong J and Chuang I L 2014 *Nano Lett.* **14** 5712

[20] Wesenberg J H, Epstein R J, Leibfried D, Blakestad R B, Britton J, Home J P, Itano W M, Jost J D, Knill E, Langer C, Ozeri R, Seidelin S and Wineland D J 2007 *Phys. Rev.* A **76** 053416

[21] Wan W, Chen L, Wu H Y, Xie Y, Zhou F and Feng M 2013 *Chin. Phys. Lett.* **30** 073701

[22] Yan L L, Wan W, Chen L, Zhou F, Gong S J, Tong X and Feng M 2016 *Sci. Rep.* **6** 21547